

Experimental Study of the Coking Phenomenon Effects on Spray Characteristics of the High Pressure Diesel Injector

M. Sheykhvazayefi^{1†}, M. Gorji-Bandpy¹, A. Hajialimohammadi² and M. Agha Mirsalim³

¹ Mechanical Engineering Department, Babol University of Technology, Babol, Iran

² Mechanical Engineering Department, Semnan University, Semnan, Iran

³ Mechanical Engineering Department, Amirkabir University of Technology, Tehran, Iran

†Corresponding Author Email: meysam.vazayefi@stu.nit.ac.ir

(Received August 30, 2019; accepted November 16, 2019)

ABSTRACT

The novel diesel engines with advanced fuel injection systems are equipped with solenoid injectors comprising multiple small nozzle orifices which makes considerable improvement in fuel spray characteristics and engine performance along with providing high pressure fuel injection system. On the other hand, poor fuel quality, impurities and heavy metal elements in the diesel fuel, and high temperature medium in the diesel engines combustion chamber lead to remarkable deposits formation in the small holes of the nozzle. In addition, it results in partial or complete nozzle hole obstruction which is called injector nozzle coking having detrimental effects on discharged spray ideal behavior and proper engine performance. In this work, the analysis of coking phenomenon influences on diesel spray macroscopic characteristics have been done. Initially, the coked injectors with different time operation and deposit amounts are prepared under experimental and specific operating conditions. Then, the images recorded from the spatial and temporal evolution of a diesel spray in various injection and chamber pressures, are processed through the extended code in MATLAB software in order to analyze discharged fuel spray characteristics. The SCHLIEREN Imaging Method with high speed camera has been utilized in a CVC (constant volume chamber) without combustion. Non-Destructive Electron Microscopy Method of SEM (Scanning Electron Microscope) imaging was utilized in order to analyze sediments quantity and construction changes during injector working in the real engine conditions. The results show that, sediments occupy 20, 40, 75 and 90% of the total hole opening surface, respectively in the injectors with 300, 700, 800 and 900 hours operating time. By increasing the injector operation time and accumulated sediment amount on the nozzle, the discharged injector spray exhibits a more inappropriate behavior. Moreover, The Results revealed that coking has considerable effects on the spray tip penetration at low injection pressures. As injection pressure increases, the decreasing rate of the penetration length alleviates gently. In other words, at high injection pressures (1500 bar and higher) the penetration length has minor drop compared with non-utilized injectors even at 900 hours operating time, but the spray projected area can be reduced up to 28% in high chamber pressures.

Keywords: Diesel engine; Nozzle coking; Schlieren imaging; Coked injector.

NOMENCLATURE

ECU	electronic control unit	t	time
P_{amb}	absolute ambient pressure	T_r	threshold value
P_{inj}	relative injection pressure		
SOI	start of injection	θ	spray cone angle
S	spray tip penetration		

1 INTRODUCTION

In recent years, utilization of the new generation of diesel engines with advanced direct fuel injection system in passenger vehicles propulsion has been

grown. Higher torque and fuel efficiency of these engines have made them suitable option (even at lower speed of the engine) in comparison with gasoline engines.

Unlike their older generation, these engines, while

maintaining engine efficiency, have been significantly effective in reducing environmental pollutants including soot, unburnt hydrocarbons and carbon dioxide (Stanly *et al.* 2017). The noise and vibration of the engine have been diminished like gasoline types (Montanaro and Allocca 2013).

Spray characteristics determine the combustion quality in diesel engines and the spray quality depends on the parameters like fuel type, injection and chamber pressures and temperatures, injector nozzle holes geometry and so on (koo *et al.* 1997; Timoney and Smith 1995).

Increasing the number of injector nozzle holes reduces each hole diameter and increases the sensitivity of the nozzle to the sediment formation (Argueyrolles *et al.* 2007). The poor fuel quality and impact of fuel spray with hot injector nozzle tip inside the high temperature combustion chamber will exacerbate the sediments formation (Klaau 2004). One important phenomenon which could change the nozzle hole geometry and spray shape is designated coking being found in various locations, such as inside the injector body and nozzle hole (Montanaro and Allocca 2013), near to the nozzle outlet or on the injector nozzle tip.

The deposits accumulated on injector nozzle results in partial or complete obstruction of nozzle holes, injector performance disruption, increasing injection duration (Stanly *et al.* 2017), fuel aggregation among formed deposit layers (Zhou *et al.* 2018) and aggravating fuel consumption (DAmbrosio and Ferrari 2012). It should be noted that, the injector nozzle deposit interaction with fuel flow through injector hole has a detrimental effect on spray characteristics discharged from injector, causing weak fuel atomization, remarkable fuel injection flow losses, incomplete combustion, emissions intensification and engine power loss (Caprotti *et al.* 2005; Leedham *et al.* 2004; Caprotti *et al.* 2010). There will be fuel flow decreases resulted by nozzle hole deposits even at the highest injection pressure and maximum applicable engine power (Ikemoto *et al.* 2011).

Numerous studies have been implemented about coking phenomenon due to the importance of this subject and its destructive effects on internal combustion engines. A group of researchers investigated the effects of this phenomenon on direct injection gasoline injectors. Based on Wen's *et al.* (2016) and Attar's *et al.* (2016) experimental studies, the deposit formation on gasoline direct injection injector nozzle indicates penetration length enhancement and spray cone angle reduction discharged from the injector. In another experimental research accomplished by Song *et al.* (2016) injector's deposits had led to cone angle and penetration length decline of the spray. The results show that the injector deposits effects on the spray characteristics are not always similar. In other words, deposits formation process in the injector would be changed in different kind of engines and sprays.

The different deposits structure accumulated over the injectors can influence the interaction between

deposits and fuel flow altering the spray characteristics discharged from the injector. Pos *et al.* (2015) and Wang *et al.* (2017a) found fundamental differences between the general spray structure discharged from the fouled and non-fouled injectors through fuel spray imaging. Song *et al.* (2016) and Wang *et al.* (2017b) investigated deposits structure of the fouled injectors via SEM method. In order to visualize the deposit inside the injector, they utilized the destructive wire cut method to approach inner deposits through cross-sectional cutting of the injector. During the cutting process, a large amount of unpredictable deposits was parted, that put uncertainty in their results. Zhou *et al.* (2018) examined the effects of interaction between deposits inside of the fouled injector and the discharged spray. They reported fuel deposition among formed sediments layers, reducing output flow, formation of ligaments and large droplets in the outlet spray and fuel aggregation on tip of the fouled injector in all tested injection pressures.

The sediment amounts formed on the new generation diesel injectors are much more than gasoline injectors because of diesel fuel nature and high temperature operating mode of the diesel engines and smaller holes of their injectors. In most studies (Arpaia *et al.* 2009; Mancaruso *et al.* 2013; Risberg *et al.* 2013; Smith and Williams 2015; Tang *et al.* 2009; Williams *et al.* 2013), some techniques for accelerating the injector deposition (such as adding zinc to diesel fuel) have been used in order to investigate its destructive effects.

Montanarou and Allocca (2013) investigated the effect of a nozzle coking (made by accelerator method) on the behavior of the discharged spray from three diesel injectors with different outflow rates. According to their findings, the nozzle sediments in all test conditions reduced the amount of outlet flow and the spray penetration length. The greatest sediment effect and increasing the output flow difference from the injector and the spray penetration length between the two fouled and non-fouled modes were reported in the injector used with lower output flow and fuel injection pressure. Napolitano *et al.* (2013) used as well three injectors with different outflow to examine the effects of nozzle coking on emissions and engine performance.

After an accelerated deposition process, reducing the amount of injector flow rate, engine power loss, increasing the engine exhaust gases temperature and heightening the amount of soot, carbon monoxide, unburned hydrocarbons and particulates were reported especially in injector with lower flow rate. Königsson *et al.* (2014) compared the sediment formation process of experimental single-cylinder diesel engine with dual diesel-gas and diesel fuel. The greatest amount of sediment was formed in engine operation with dual diesel-gas fuel and lower fuel injection pressure. Based on their studies of the engine's performance with diesel fuel, the constructed deposit volume was less and was more rugged due to the high volume of travelling fluid and the formation of cavitation and stronger shear

Table 1 Dimensional parameters of the nozzle orifices

orifice number	1	2	3	4	5	6	7	8
α°	76	76	76	76	76	76	76	76
β°	43	88	133	178	223	268	313	358
$d_0(mm)$	0.12	0.12	0.12	0.12	0.12	0.12	0.12	0.12

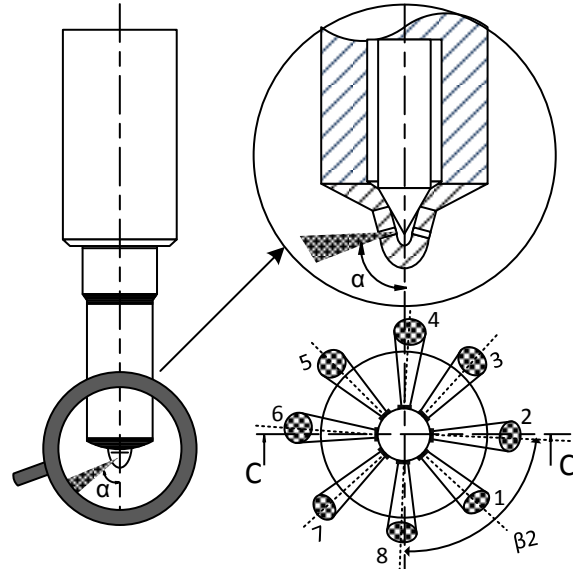


Fig. 1. Injector nozzle schematic.

force inside the hole. Whilst, the sediment volume and surface was much further and smoother in this case due to the high operating temperature of the engine with dual diesel-gas fuel.

Stanly *et al.* (2017) utilized injectors with much coking sediments formed in public vehicles application over time. Having injectors wiped off with a commercial sediment eliminating solvent, Lower specific fuel consumption and shorter injection time were reported. Moreover, they related fuel atomization improvement, uniformity of multiple injection jets and outgoing fuel stream enhancement of injector nozzle holes after fuel system deposition process.

As mentioned earlier, in most studies, the researchers developed a sediment deposition in diesel injector nozzle by adding zinc and using accelerator techniques (Arpaia *et al.* 2009; Mancaruso *et al.* 2013; Risberg *et al.* 2013; Smith and Williams 2015; Tang *et al.* 2009; Williams *et al.* 2013). As in these works the fuel specification is not the same as the standard diesel fuel, in the present work, in order to properly investigate the deposition phenomenon, the test conditions are selected in normal engine operation with standard fuel. The injectors after specified durations (300, 700, 800 and 900 hours) from start of test was investigated in order to measure sediments quantity and construction and discharged spray characteristics including penetration length, cone angle, spray projected area and spray average velocity.

Another novelty of this work that was not reported

before, was investigation of fuel spray characteristics in various injection and chamber pressures with fouled diesel injector in real engine working conditions and standard fuel.

2 MATERIALS AND METHODS

2.1 Injectors

The solenoid injectors used in this work is made by Bosch Germany (CRI2.2 model) and its nozzle is of SAC type containing 8 holes with identical diameter whose schematic design and dimensional parameters have been provided in Fig. 1 and Table 1.

α is a diagonal angle inclining to downwards between outlet sprays axes and injector horizontal axes and β is a transverse angle between outlet sprays axes and injector vertical axes.

2.2 Deposition Process of the Injector Nozzle

In previous studies, the fouled injector under real operating conditions of vehicle had been used to investigate the deposit effects on the spray behavior discharged from the injector. The results had a very low reliability and accuracy due to the impossible accurate engine and injector operating conditions recording in different speeds and torques and deposition conditions uncertainty of the injectors. Moreover, the deposition process of diesel injector was accelerated in prior researches by adding zinc element to the diesel fuel which increased

inaccuracy rate of the deposition process with respect to the fuel mixture and zinc homogeneity and non-monotonous zinc distribution in diesel fuel.

Therefore, in this research, the injector deposition process has been experimentally implemented in order to scrutinize injector nozzle deposits impact on fuel spray characteristics and injector performance. The diesel fuel with specifications stated in the table 2 has been used without incorporating zinc element. In spite of test time and experiments cost increase, the results will be nearly identical to real engine operational conditions. The deposition process was performed in the engine test bench (Fig. 2) with an EFD commercial diesel engine and a Bosch-CRI2.2 injector mounted on it which its specifications have been provided in Table 3. An indirect AVL flow dynamometer was used in order to control engine's speed and torque which plays an acceleration pedal role in real engine operational condition.

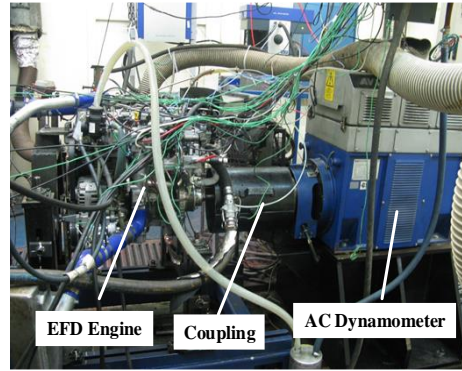


Fig. 2. EFD engine test room.

Table 2 Diesel fuel characteristics

Parameter	Value	Test Method
Viscosity (mm^2/s at 40°C)	2.99	ASTM D445
Density (kg/m^3 at 15 °C)	828	ASTM D4052
Flash Point (°C)	62	ASTM D93
Sulfur concentration (ppm)	30.2	ASTM D4294
Cetane number	54.0	ASTM D976

The deposition process was carried out based on the endurance test cycle shown in Fig.3. The endurance cycle duration is 15 minutes. This cycle was repeated until 300 hours of engine operational duration (1200 cycles). At this point, the 1th injector was dismantled. The same procedure was carried out for 2th, 3th and 4th injectors at 700,800, and 900 hours from the test starting.

Table 3 EFD engine technical specification

Engine type	In-line 4 cylinders-diesel commercial
aspiration	VGT turbocharger
Bore/stroke	76mm/82.5mm
Displacement volume	1.5 lit
Compression ratio	16.5
Injection system	Common-rail
Max. power	90KW@4000rpm
Max. torque	256N.m@ 2600 rpm

This method was chosen owing to high susceptibility and brittleness of deposits formed on injector nozzle tip and inadvertent breaking off possibility of the deposits during frequent injector assembling and disassembling.

2.3 SCHLIEREN Imaging Process of Fuel Spray

The experimental facilities are comprised of stainless steel (CVC) which has a diameter and length of 13cm. Two sides of the chamber have been equipped with transparent windows made of quartz having a thickness and diameter of 8cm and 16cm respectively to provide optical transmission path aligned with imaging orientation which is shown in Fig. 4. More information about the SCHLIEREN imaging system can be found in (Erfan *et al.* 2017).

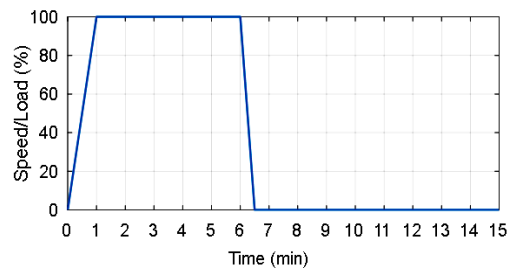


Fig. 3. Endurance test cycle in order to injector coking attainment.

The chamber would be able to withstand pressures up to 100bar. The CVC inner gas feeding system are used in order to enhance the interior pressure of the chamber up to 10 bar (Hajjalimohammadi *et al.* 2012).

This system includes of 20Mpa nitrogen gas tank, gas transmission pipes into the tank, pressure control valves and digital indicators of chamber pressure which is utilized to alter the gas composition inside of the chamber and regulate the pressure to the desired extent.

The utilized fueling system in this project is a common rail system. In order to analyze actual performance of the EFD diesel engine, the main components of this system (high pressure pump and injector) have been selected from the EFD engine. The system comprises of electromotor, high pressure pump, fuel rail, high pressure pipes, fuel injector fuel tank, low pressure pump and inverter (Mohebbi *et al.* 2016). The Bosch-CP4.1 high pressure pump driven by A.B.B electrical motor is a

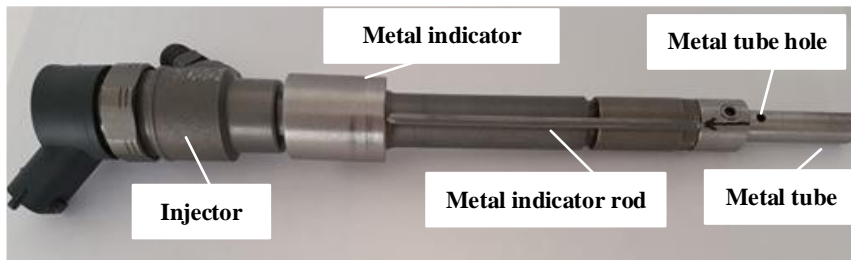


Fig. 5. Diesel injector.

one-cylinder pump which is able to create pressure amounts up to 2000 bar inside the fuel common rail. With respect to constant speed of the electromotor, its velocity and high pressure pump regulation are controlled via 3-phase LG5A inverter. The inverter generates a minimum power loss of the engine's nominal mode through changing the voltage and frequency simultaneously. The pressure control, fuel injection duration, electromotor speed, as well as imaging start time determination are carried out by the electronic control unit. This unit controls the fuel pressure fluctuations in the common fuel rail, so that the results of the fuel injection would have a high accuracy. At this stage, the diesel fuel with the specifications given in Table 2 has been used. The test conditions are fully presented in Table 4.

Table 4 Test conditions

P_{inj} (bar)	500, 1000, 1500
P_{amb} (bar)	0.87, 10.87
Ambient Temperature (K)	293
Injection duration (ms)	2-3
Nozzle hole diameter (mm)	0.12

In order to image and examine the discharged spray characteristics specified on the injector nozzle, a metal tube according to the Fig. 5 is mounted on the injector to allow the desired spray to flow from the hole of the injector. The exhausted sprays from the other 7 holes after colliding with interior wall of the metal tube flow to the bottom of the metal chamber. More specification about the injector adaptor can be found in (Sohrabiasl *et al.* 2017).

Moreover, due to sedimentation of the nozzle after long engine operational times and unrecognizable target hole, the metal part is designed and manufactured with an indicator according to the injector body structure as can be seen in Fig. 5. This metal indicator will significantly help the target fouled hole to be located in front of the metal tube hole and lead to laboratory error reduction. In this research, the SCHILLERIN method is implemented for the output fuel spray imaging as shown in Fig. 6.

In this system, the light is emitted from a halogen lamp as a point source. The output spot light collides with the first mirror with focal length of 2610 mm. Next, the reflected light cluster from the first mirror passes through CVC and then is hit to the later mirror with focal length of 2570 mm in parallel rays. Finally, the reflected rays of the

second mirror are converted to a spot light. It enters the camera in the wake of the travelling through the sharp edge and the image of the spray shadow is depicted as a result. The sharp edge role is to reduce the disturbances which are existed inside the camera and before its lens. A fast CMOS cube3 camera of Motion Blitz corporation has been utilized for imaging process. The camera speed reaches up to 120,000 frames per second. Its maximum image resolution (512×512 pixels) is 2500 frames per second, and the lens used in this camera is an AF Nikon 70-300 mm. The image resolution is adjustable by the camera. Obviously, the higher the photo resolution, the lower the imaging speed. The imaging speed in this research was 17316 frames per second in 74×160 of resolution.

2.4 Image Processing Method

The necessity of examining various spray characteristics during the test, the 10-time repetition of each test and the high number of images stored in different test modes require an algorithm that can analyze the number of images with high speed and precision., therefore the modified version of the code provided in the (Hajjalimohammadi *et al.* 2013, 2016) has been developed to analyze the images in MATLAB software.

In this code, a subtractive image processing algorithm is used to obtain the spray characteristics. It means that the background image will be subtracted from spray image momentarily at the beginning of the analysis. This will eliminate persistent elements of the image, such as dust particles on the mirrors, optical glasses or camera lens, and other disturbances which are present in all images, hence the remaining image only depicts a fuel spray.

In all experiments, the camera's imaging speed was adjusted to 17,316 frames per second, resulting 160×74 number of pixels in each image. The number of pixels in each image depends on the camera's imaging speed, which means the higher capturing speed, the fewer number of pixels. In order to pinpoint the spray edges, the edge detection canny standard pattern has been used (Canny 1986). In this method, the spray boundary edges are found out by specifying the maximum value of the image local gradient. The image gradient is calculated by the Gaussian function differential.

The method includes of applying the Gaussian differential function to the image. The outcome is converted to a binary image according to a

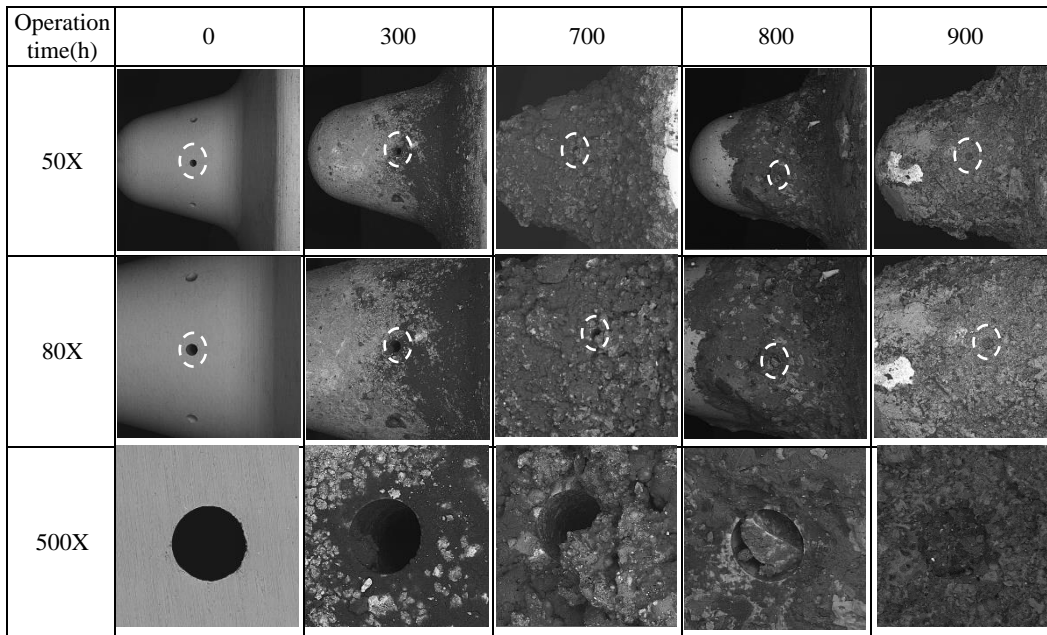


Fig. 7. The SEM images of the injector nozzle tip with different operational duration and magnification of 50, 80, 500x.

threshold value. The points where the Gaussian function differential is greater than the determined threshold value is considered 1 (white spots) and the others equal to zero (black spots). This high-efficiency method is used in images with a high degree of disturbance, detecting the weakest edges with rational probability. Edge detection approach is sensitive to selection of an appropriate threshold value. In other words, if the threshold value is assigned a small amount consequently, the edges will emerge outside of the spray. On the other hand, considering high amount of the threshold value leads to the edge detection quality decline exclusively in dilute fuel regions. $Tr = 0.06$ is the most appropriate threshold value for spray precise edge detection which has been used to analyze the spray photos.

The results illustrate that the threshold value alteration will impress penetration length up to 4% which could be reasonable error in experimental method. The binary image is monitored from the dark end of the image to the top till reaching to first white pixel in order to calculate the spray penetration length through the MATLAB code. As a result, this point is considered as a leading point. The distance between this point and the outlet point of the spray (in the direction of the spray axis) is calculated then multiplied by the image scale factor to obtain the penetration length. Numerical differentiation of the spray penetration graphs obtained at the peculiar time of spraying provides the injector tip speed.

The spray edge velocity is computed by division of its traveled distance into required time duration. The interval between two consecutive images is 0.05775 ms according to the capturing velocity. In accurate terms, the spray velocity calculated by

MATLAB code is the average velocity of spray edge between two successive images.

In order to spray area determination, the gray image resulted by background image subtraction from spray image is converted to a binary image by Otsu's method (Hajjalimohammadi *et al.* 2014). Finally, having been multiplied the number of white pixels in the square of the scale factor, the amount of the spray projected area will be yielded.

3 RESULTS AND DISCUSSION

In this section, at first, the substances and structure of the sediment formed on injector nozzles will be analyzed. Then, the sediment influences will be investigated on macroscopic spray characteristics such as penetration length, cone angle, average velocity and spray projected area in different injection and ambient pressures.

3.1 Analysis of Deposits Characteristics

Fig. 7 illustrates the SEM images of the injector nozzle tip after different engine operational times. Initially, the surface and holes of the new injector nozzle tip are clean and free of any clogging sediment. As the injector operational time increases up to 300 hours, the sediment gradually accumulates on the nozzle tip surface dispersedly with a small thickness and on a part of the nozzle hole opening up to a maximum 40 Microns. The sediments formed in the hole opening extends up to 20% of the hole entrance and the fundamental sediment is not formed inside the hole.

The sediment quantity on the nozzle tip surface and nozzle hole will be gently increased as the injector operational time increases up to the 700h. The

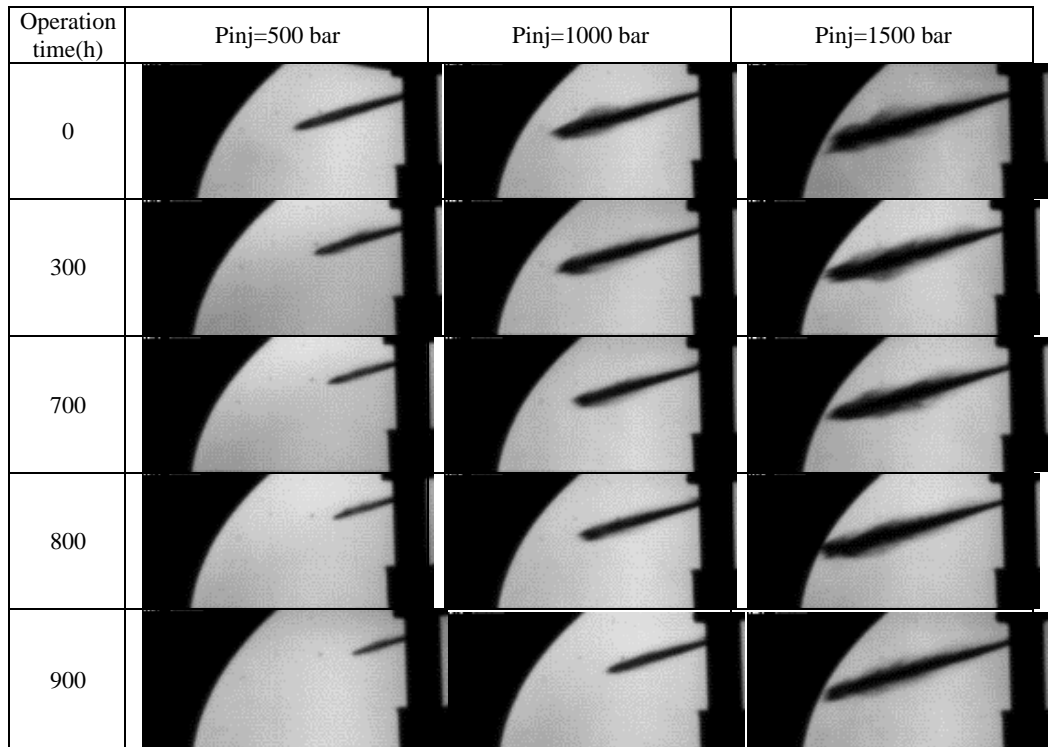


Fig. 8. Diesel spray images of injectors with various operational duration at 0.288 ms after SOI and $P_{amb} = 0.87 \text{ bar}$

deposits are remarkably formed on a part of the hole opening up to 62 Micron and around the hole occupying at least 40% of the hole opening area. An increase in injector operational time to 800 hours results in more sediment accumulation beside the former sediments, accelerating sedimentation process and increasing the amount of sediments, especially at the nozzle hole entrance. The sediments thickness has expanded to 110 Microns in a part of the openings and accounts for at least 75% of the total surface area of the openings. A 100h operation time difference compared to the prior state, indicates sediment formation development towards saturation mode. The deposit formation process intensively continues in the course of the injector operation. The injector will roughly approach to the saturation mode in 900h operational duration. At this point, the deposits are uniformly extended with considerable thickness on the injector nozzle tip surface and the nozzle hole filling nearly the entire hole opening space of the hole, with the exception of some areas around the edge of the hole opening (equivalent to 90% of the opening hole).

3.2 The Injectors Spray Behavior Analysis

The spray images of injectors with different operational duration have been depicted in Fig. 8 at 0.288 ms after SOI (spray collision instant with wall for new injector at $P_{inj}=1500 \text{ bar}$) for determined injection pressures and ambient pressure of 0.87bar.

It was observed from images that the output spray from utilized injectors has a slight fuel injection delay (0.03 ms) even in 900-hour operation time at

1500 bar injection pressure due to the high fuel pressure and fuel flow dominance over sediments inside the nozzle hole. Moreover, the injectors outlet spray with different operating times simultaneously reach to the combustion chamber wall at $P_{inj}=1500 \text{ bar}$. The output spray of injectors with 300, 700, 800, 900 hours operating times approach the wall by 0.029, 0.087, 0.116, 0.173ms time delay compared with free spray at 1000 bar injection pressure.

By reducing the injection pressure to 500 bar and increasing the resistance of the nozzle hole sediments to the fuel flow, the injection delay will increase as well. In other words, the delay time for fouled injectors with 300, 700, 800, 900-hour operational duration are 0.12, 0.2, 0.26, 0.35 ms respectively compared with non-utilized injector.

It can be inferred by comparing the spray penetration lengths at 0.51 ms after SOI from Fig. 9 that the penetration lengths with 300, 700, 800 and 900 hours operational times of injectors have experienced an average decrease of 9, 13, 16 and 19% compared with new injector with injection and chamber pressures of 500 and 0.87 bar respectively.

As injection pressure is elevating, the role of the injector deposits fades in weakening of spray penetration.

In other words, as illustrated in Fig.10, as injection pressure increases to 1000 bar, the penetration length reduction of fouled injectors will be decreased in comparison with injection pressure of 500 bar.

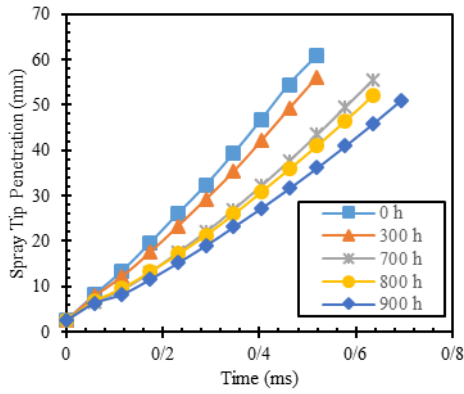


Fig. 9. Spray penetration length discharged from the injectors with operational duration versus time at $P_{inj} = 500 \text{ bar}$ and $P_{amb} = 0.87 \text{ bar}$.

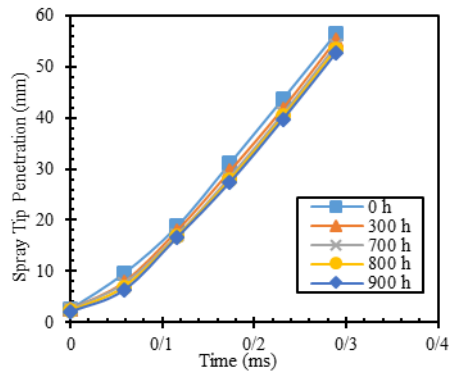


Fig. 11. Spray penetration length discharged from the injectors with operational duration versus time at $P_{inj} = 1500 \text{ bar}$ and $P_{amb} = 0.87 \text{ bar}$.

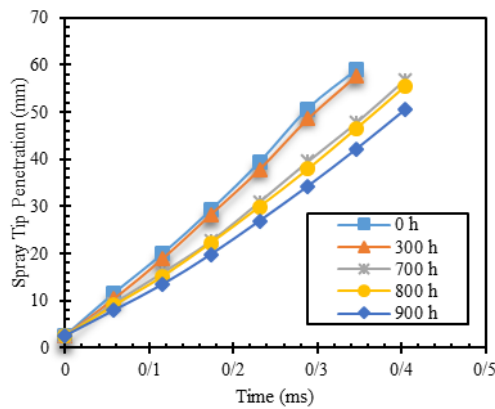


Fig. 10. Spray penetration length discharged from the injectors with operational duration versus time at $P_{inj} = 1000 \text{ bar}$ and $P_{amb} = 0.87 \text{ bar}$.

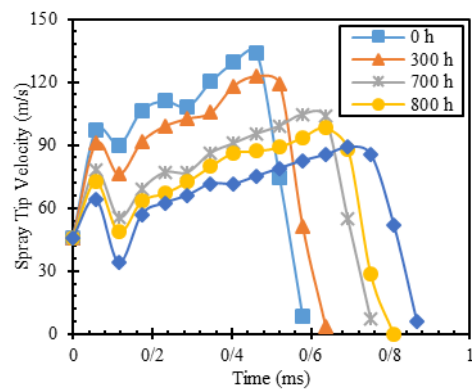


Fig. 12. Spray average tip velocity discharged from injectors with different operation time versus time at $P_{inj} = 500 \text{ bar}$ and $P_{amb} = 0.87 \text{ bar}$.

Moreover, as shown in Fig.11 in injection pressure of 1500 bar the difference between penetration lengths of new and fouled injectors is minor and even after 900 hours working, the penetration is approximately not changed compared with new injector.

As for passenger car diesel engine in some operating modes like cold start, low speeds and torques, injection pressures are not in the range of maximum injections (1500 bar for this engine type), power loss and increase in fuel consumptions of engine is predictable with these results. It should be noted also that the penetration of spray is not the only parameter in characterization of the spray, another important parameter is the spray angle that determine the mixture formation quality of the spray. As shown in Fig. 8, it is true that the penetration of spray is not changed much in injection pressure of 1500 bar, but the spray angle is decrease considerably after 800 hours working of injector. The spray angle investigation in the current work was performed with spray projection area that could be more explained in the following sections.

The spray average velocity for injectors with different working times have been illustrated in Figs. 12-14 in $P_{amb}=0.87 \text{ bar}$ and injection pressures of 500, 1000 and 1500 bar.

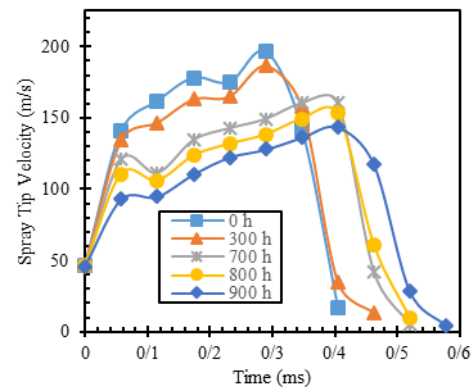


Fig. 13. Spray average tip velocity discharged from injectors with different operation time versus time at $P_{inj} = 1000 \text{ bar}$ and $P_{amb} = 0.87 \text{ bar}$.

According to velocity curves, the injected fuel flow collision with formed deposits is intensified in all injection pressures by increasing injector working time and deposit content of the nozzle. It leads to flow kinetic energy loss and spray velocity devaluation. It can be derived from Fig's 12-14 also spray edge velocity for all conditions has a peak value. This peak correspond to the injector opening time and the time of the peak velocity increases with increase of injector working hours, that reflects the fact of injector opening delay because of the

coking phenomenon. The velocity drop after peak could be due to the spray propagation in radial direction.

As injection pressure increases, the injected fuel flow passes through accumulated deposits with high power and kinetic energy. Therefore, the spray velocity discharged from utilized injector experiences further drop in comparison with non-utilized injector at higher pressures. It should be noted that, the speed disparity of injectors with different time operation has been lessened. It can be concluded that the speed difference has been notably decreased at 1500 bar injection pressure making profiles closer to each other (compared with lower injection pressures).

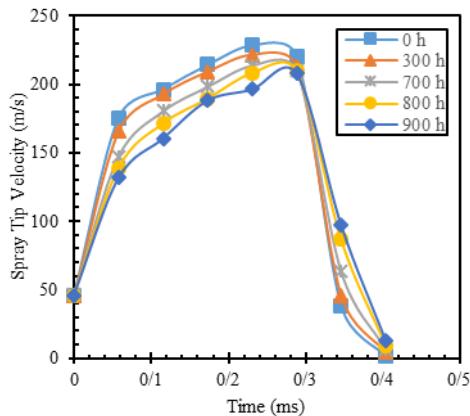


Fig. 14. Spray average tip velocity discharged from injectors with different operation time versus time at $P_{inj} = 1500$ bar and $P_{amb} = 0.87$ bar.

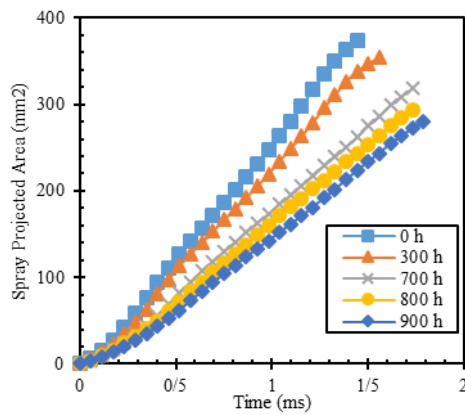


Fig. 15. Spray projected area discharged from the injectors with various operational duration versus time at $P_{inj} = 500$ bar and $P_{amb} = 10.87$ bar.

Figures 15-17 represent the spray projected area of injectors with different operational duration at $P_{amb}=10.87$ bar. As mentioned before, spray projected area represents the mixing quality of the air-fuel mixture in direct injection engines.

According to the results provided in Fig. 15, average decrease percentage of the spray projected area for injectors with 300, 700, 800,

900 working hours are 7, 16, 23, 28 percent compared with new injector. The devaluation rate calculated as the average difference between fouled and new injector spray projected area in all times that images of spray captured before collision to the CVC wall.

Moreover, the average decrease percentages of spray projected areas are 6, 13, 22, 27 and 3, 12, 19, 22 for 1000 and 1500 bar of injection pressures respectively. With respect to Figs. 15-17, It can be derived that with increasing the injection pressure, the spray projected area curves for various operating times become closer to each other.

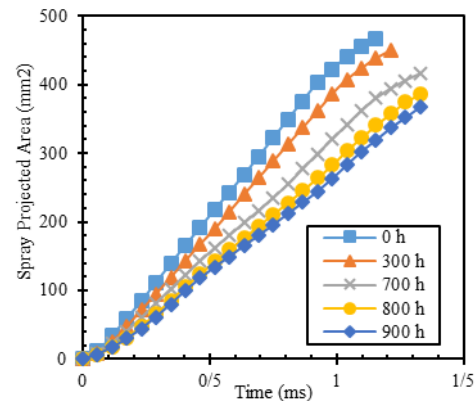


Fig. 16. Spray projected area discharged from the injectors with various operational duration versus time at $P_{inj} = 1000$ bar and $P_{amb} = 10.87$ bar.

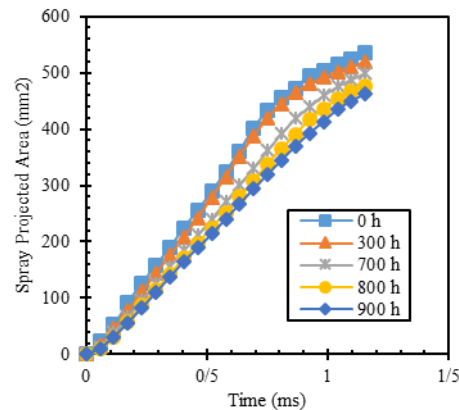


Fig. 17. Spray projected area discharged from the injectors with various operational duration versus time at $P_{inj} = 1500$ bar and $P_{amb} = 10.87$ bar.

Figures 18- 19 show the output spray of injectors with various working times at different injection and ambient pressures. The corresponding cone angles are calculated by the image processing code. As expected, enhancing injection and chamber pressures increases spray cone angle discharged from utilized injectors. The injector nozzle deposits decrease the injector output flow and spray cone angle in all injection and ambient pressures. The spray cone angle experiences further reduction as the sediment amount of the nozzle and injector operating time increase. On the other hand, by increasing the injection pressure, the destructive effects of sediments on the output spray behavior

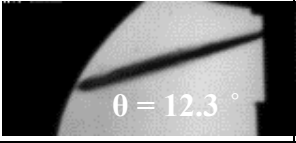
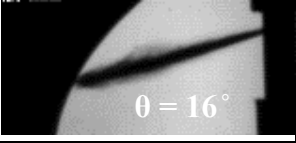
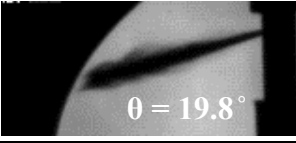
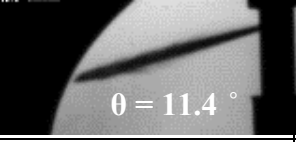
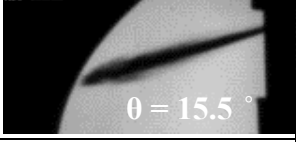
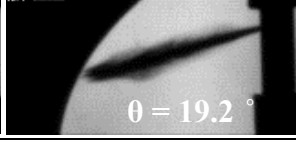
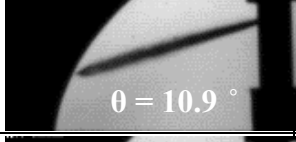
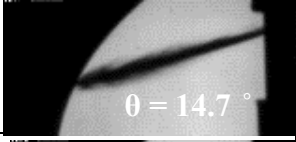
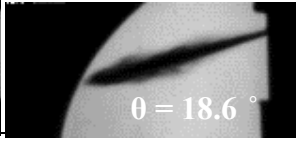
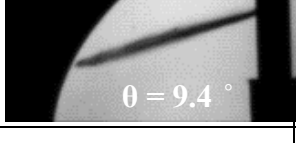
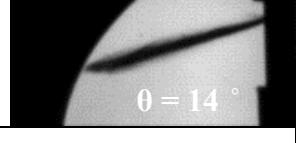
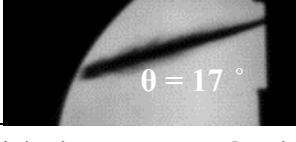
Operation time(h)	Pinj=500 bar	Pinj=1000 bar	Pinj=1500 bar
0	 $\theta = 12.3^\circ$	 $\theta = 16^\circ$	 $\theta = 19.8^\circ$
300	 $\theta = 11.4^\circ$	 $\theta = 15.5^\circ$	 $\theta = 19.2^\circ$
700	 $\theta = 10.9^\circ$	 $\theta = 14.7^\circ$	 $\theta = 18.6^\circ$
800	 $\theta = 9.4^\circ$	 $\theta = 14^\circ$	 $\theta = 17.6^\circ$
900	 $\theta = 8.8^\circ$	 $\theta = 13.3^\circ$	 $\theta = 17^\circ$

Fig. 18. Spray cone angle in verge of colliding with the wall for different injection pressures and various operational duration ($P_{amb} = 0.87 \text{ bar}$).

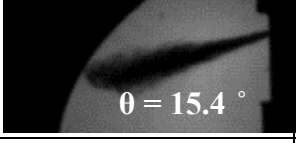
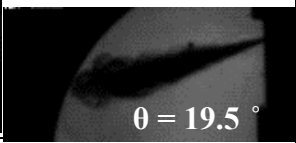
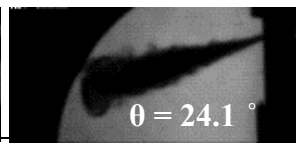
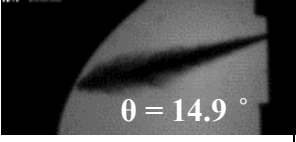
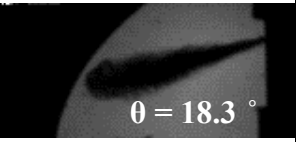
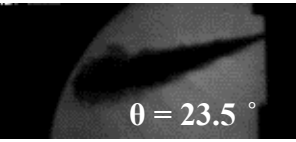
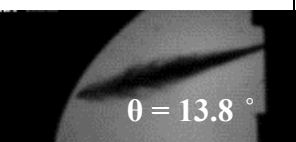
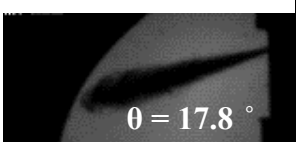
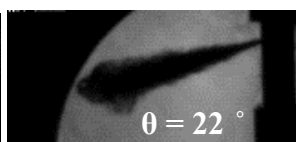
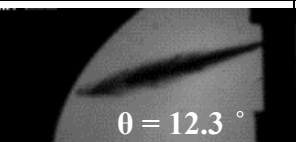
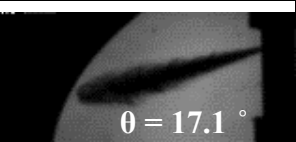
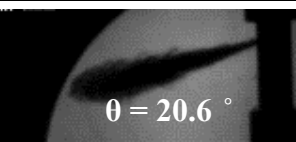
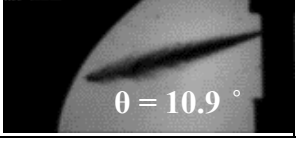
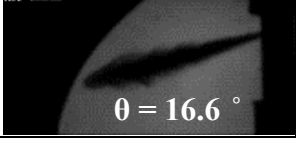
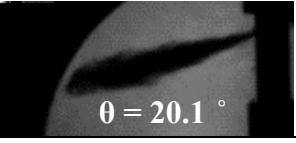
Operation time(h)	Pinj=500 bar	Pinj=1000 bar	Pinj=1500 bar
0	 $\theta = 15.4^\circ$	 $\theta = 19.5^\circ$	 $\theta = 24.1^\circ$
300	 $\theta = 14.9^\circ$	 $\theta = 18.3^\circ$	 $\theta = 23.5^\circ$
700	 $\theta = 13.8^\circ$	 $\theta = 17.8^\circ$	 $\theta = 22^\circ$
800	 $\theta = 12.3^\circ$	 $\theta = 17.1^\circ$	 $\theta = 20.6^\circ$
900	 $\theta = 10.9^\circ$	 $\theta = 16.6^\circ$	 $\theta = 20.1^\circ$

Fig. 19. Spray cone angle in verge of colliding with the wall for different injection pressures and various operational duration ($P_{amb} = 10.87 \text{ bar}$).

are decreased alleviating the spray cone angle drop discharged from utilized injectors (compared with non-utilized injector).

3.3 Experimental Results Uncertainty Analysis

The experimental results are always associated with errors. A part of them is due to equipment faults used in the tests and the rest is resulted from the human mistakes. The main sources of uncertainty in the measured data in the experimental tests of current work are irregular behavior of spray needles rise, unrepeatability, turbulent behavior of the spray, random distribution of sediments formed inside of the nozzle hole and human errors in tests implementation and image processing. A large number of the image processing errors is referred to the sensitivity of edge detection method. The blurred image and smeared marks unconformity of the optical system, increase measurement uncertainty of the spray edge location. The highest difference between the average penetration length and the measured penetration lengths of the spray has been depicted in Fig. 20 for 10 repetitions at a relative injection pressure of 500 bar and absolute chamber pressure of 10.87 bar. According to the results, the uncertainty is obtained in the range of ± 0.23 -1.1 mm and ± 1 -5 % in terms of percentage amount with 95% confidence level at different fuel injection times. This uncertainty represents the statistical variance of the moment-to-moment displacement of the spray edge for the injector and commercial refueling system used in these tests and shows repeatability of results.

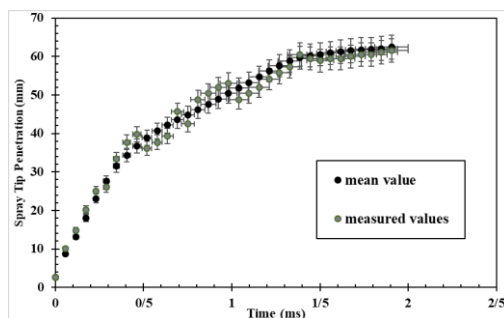


Fig. 20. Highest spray penetration length at 10 test repetition compared of the average spray penetration length for the spray pressure of 500 bar and chamber pressure of 10.87 bar.

4 CONCLUSIONS

The sediments resulted from the coking phenomenon in injectors nozzle have a very destructive effect on the ideal behavior of the output fuel spray. The fuel spray characteristics play a substantial role in internal combustion engines functional parameters like power, torque and fuel consumptions and the change in fuel spray characteristics could change these parameters. Therefore, the spray macroscopic characteristics were examined completely in this study including penetration length, cone angle, projected area and

spray average velocity for injectors with different working times with standard diesel fuel. For this purpose, the images of the spray discharging from new and fouled injectors in different conditions (taken by high speed SCHLIEREN optical method) were analyzed. Moreover, SEM Non-Destructive Optical Microscopy method was used to analyze thoroughly sediment construction and further examination of sediment interaction with injector fuel flow.

Penetration of spray tip was found to be very sensitive to the extent of nozzle sediments and the injection pressure. High quantity of sediments and low injection pressure could decrease the spray tip penetration. For instance, for nozzle with 900 hours operation with high quantity of sediments and injection pressure of 500 bar the spray penetration is 19% lower than the penetration of spray with new injector. Increasing the injection pressure could decrease the sensitivity of the spray penetration to the injector coking. The spray projected area is more sensitive to the sediment formation in all injection pressures, which means that the weak mixture formation is the most important effect of the injector coking phenomenon. Decrease in the spray projected area could be maximum 28% in case of the injector with sediments.

For the diesel fuel tested in the present work, As the operating time of the injector increases, the amount of sediment level of the nozzle tip and the nozzle opening are gradually increased. Based on the SEM images taken from the nozzle tip at 300, 700, 800, and 900 hours of injector, the sediments cover about 20, 40, 75 and 90 percent of the opening hole surface. Then, the sedimentation process will be saturated approximately in the 900-hours operating time of the injector.

ACKNOWLEDGEMENTS

The authors would appreciate the Iran Khodro Power train Company (IPCO) for financial support. This research was carried out in laboratory facility of this company.

REFERENCES

- Argueyrolles, B., S. Dehoux, P. Gastaldi, L. Grosjean, F. Levy, A. Michel and D. Passerel (2007). Influence of injector nozzle design and cavitation on coking phenomenon. *SAE*, 2007-01-1896.
- Arpaia, A., A. E. Catania, S. D. Ambrosio, A. Ferrari, S. P. Luisi and E. Spessa (2009). Injector Coking Effects on Engine Performance and Emissions. *Internal Combustion Engine Division Fall Technical Conference, ASME*, 229-241.
- Attar, M. A., T. Badawy and H. Xu (2016). Assessment of gasoline direct injector coking effects on spray dynamics and fuel atomization. *SAE*, 2016-01-2192.
- Canny, J. (1986). A computational approach to edge

- detection. *IEEE Trans Pattern Anal Mach Intell* PAMI-8(6), 679–698.
- Caprotti, R., A. Breakspear, O. Graupner and T. Klaua (2005). Detergency Requirements of Future Diesel Injection Systems. *SAE*, 2005-01-3901.
- Caprotti, R., N. Bhatti and G. Balfour (2010). Deposit Control in Modern Diesel Fuel Injection Systems. *SAE* 3(2), 901-915.
- DAmbrosio, S. and A. Ferrari (2012). Diesel Injector Coking: Optical-Chemical Analysis of Deposits and Influence on Injected Flow-Rate, Fuel Spray and Engine Performance. *Journal of Engineering for Gas Turbines and Power, Transactions of the ASME* 134(6), 062801-2.
- Erfan, I., A. Hajjalimohammadi, I. Chitsaz, M. Ziabasharhagh and R. J.Martinuzzi (2017). Influence of chamber pressure on CNG jet characteristics of a multi-hole high pressure injector. *Fuel* 197, 183-193.
- Hajjalimohammadi, A., D. Edgington-Mitchell, D. Honnery, N. Montazerin, A. Abdullah and M. Agha Mirsalim (2016). Ultra high speed investigation of gaseous jet injected by a single-hole injector and proposing of an analytical method for pressure loss prediction during transient injection. *Fuel*, 184, 100–109.
- Hajjalimohammadi, A., D. Honnery, A. Abdullah and M. Agha Mirsalim (2013). Time resolved characteristics of gaseous jet injected by a group-hole nozzle. *Fuel* 113, 497–505.
- Hajjalimohammadi, A., D. Honnery, A. Abdullah and M. Agha Mirsalim (2014). Sensitivity analysis of parameters affecting image processing of high pressure gaseous jet images. *The Journal of Engine Research* 33, 43-52.
- Hajjalimohammadi, A., S. AhmadiSoleymani, A. Abdullah, O. Asgari and F. Rezai (2012). Design And Manufacturing of A Constant Volume Test Combustion Chamber For Jet And Flame Visualization of CNG Direct Injection, *Applied Mechanics and Materials*, 217-219, 2539-2545.
- Ikemoto, M., K. Omae, K. Nakai, R. Ueda, N. Kakehashi and K. Sunami (2011). Injection Nozzle Coking Mechanism in Common-rail Diesel Engine. *SAE*, 2011-01-1818.
- Klaua, T. (2004). Impact of fuel additives on Diesel injector deposits. *SAE*, 2004-01-2935.
- Königsson, F., P. Risberg and H. Angstrom (2014). Nozzle Coking in CNG-Diesel Dual Fuel Engines. *SAE*, 2014-01-2700.
- Koo, J., S. Hong, J. Shakal and S. Goto (1997). Influence of Fuel Injector Nozzle Geometry on Internal and External Flow Characteristics. *SAE* 106(3), 568-580.
- Leedham, A., R. Caprotti, O. Graupner and T. Klaua (2004). Impact of Fuel Additives on Diesel Injector Deposits. *SAE*, 2004-01-2935.
- Mancaruso, E., L. Sequino, B. Vaglieco and C. Ciaravino (2013). Coking Effect of Different FN Nozzles on Injection and Combustion in an Optically Accessible Diesel Engine. *SAE*, 2013-24-0039.
- Mohebbi, M., A. Abdul Aziz, A. Hamidi, A. Hajjalimohammadi and V. Hosseini (2016). Modeling of pressure line behavior of a common rail diesel engine due to injection and fuel variation. *Journal of the Brazilian Society of Mechanical Sciences and Engineering* 39, 3, 661-669.
- Montanaro, A. and L. Allocca (2013). Impact of the Nozzle Coking on Spray Formation for Diesel Injectors. *SAE*, 2013-01-2546.
- Napolitano, P., Ch. Guido, C. Beatrice and C. Ciaravino (2013). Analysis of Nozzle Coking Impact on Emissions and Performance of a Euro5 Automotive Diesel Engine. *SAE*, 2013-24-0127.
- Pos, R., R. Cracknell and L. Ganippa (2015). Transient characteristics of diesel sprays from a deposit rich injector. *Fuel* 153(2), 183–191.
- Risberg, P., L. Adlercreutz, M. Aguilera, T. Johansson, L. Stensiö and H. Angstrom (2013). Development of a Heavy Duty Nozzle Coking Test. *SAE*, 2013-01-2674.
- Smith, A. and R. Williams (2015). Linking the Physical Manifestation and Performance Effects of Injector Nozzle Deposits in Modern Diesel Engines. *SAE* 8(2), 344-357.
- Sohrabiasl, I., M. Gorji-Bandpy, A. Hajjalimohammadi and M. Agha Mirsalim (2017). Effect of open cell metal porous media on evolution of high pressure diesel fuel spray. *Fuel*, 206, 133–144.
- Song, H., J. Xiao, Y. Chen and Z. Huang (2016). The effects of deposits on spray behaviors of a gasoline direct injector. *Fuel* 180, 506–513.
- Stanly, R., G. Parameswaran and R. Rajkiran (2017). Effect of Fuel System Coking on Vehicle Performance and Spray Field. *SAE*, 2017-01-5017.
- Tang, J., S. Pischinger, M. Lamping and T. Korfer (2009). Coking Phenomena in Nozzle Orifices of DI- Diesel Engines. *SAE* 2(1), 259- 272.
- Timoney, D. and W. Smith (1995). Correlation of Injection Rate Shapes with D.I. Diesel Exhaust Emissions. *SAE* 104(4), 162-170.
- Wang, Z., X. Ma, Y. Jiang, Y. Li and H. Xu (2017a). Influence of deposit on spray behavior under flash boiling condition with the application of closely coupled split injection strategy. *Fuel* 190, 67–78.
- Wang, B., T. Badawy, Y. Jiang, H. Xu, A. Ghafourian and X. Zhang (2017b). Investigation of deposit effect on multi-hole injector spray characteristics and air/fuel mixing process. *Fuel* 191, 10–24.

- Wen, Y., Y. Wang, C. Fu, W. Deng, Z. Zhan, Y. Tang, X. Li, H. Ding and S. Shuai (2016). The impact of injector deposits on spray and particulate emission of advanced gasoline direct injection vehicle. *SAE*, 2016-01-2284.
- Williams, R., A. Smith and I. Buttery (2013). Formation and Removal of Injector Nozzle Deposits in Modern Diesel Cars. *SAE* 6(1), 230-240.
- Zhou, J., Y. Pei, Z. Peng, Y. Zhang, J. Qin, L. Wang, C. Liu and X. Zhang (2018). Characteristics of near-nozzle spray development from a fouled GDI injector. *Fuel* 219, 17–29.